J. Membrane Biol. 83, 157–167 (1985)

The Journal of
Membrane Biology

Junctional Transfer in Cultured Vascular Endothelium: II. Dye and Nucleotide Transfer

David M. Larson* and Judson D. Sheridan
Zoology Program and Department of Anatomy, University of Minnesota, Minneapolis, Minnesota 55455

Summary. Vascular endothelial cultures, derived from large vessels, retain many of the characteristics of their *in vivo* counterparts. However, the observed reduction in size and complexity of intercellular gap and tight junctions in these cultured cells (Larson, D.M., and Sheridan, J.D., 1982, *J. Cell Biol.* **92**:183) suggests that important functions, thought to be mediated by these structures, may be altered *in vitro*. In our continuing studies on intercellular communication in vessel wall cells, we have quantitated the extent of junctional transfer of small molecular tracers (the fluorescent dye Lucifer Yellow CH and tritiated uridine nucleotides) in confluent cultures of calf aortic (BAEC) and umbilical vein (BVEC) endothelium. Both BAEC and BVEC show extensive (and quantitatively equivalent) dye and nucleotide transfer. As an analogue of intimal endothelium, we have also tested dye transfer in freshly isolated sheets of endothelium. Transfer in BAEC and BVEC sheets was more rapid, extensive and homogeneous than in the cultured cells, implying a reduction in molecular coupling as endothelium adapts to culture conditions. In addition, we have documented heterocellular nucleotide transfer between cultured endothelium and vascular smooth muscle cells, of particular interest considering the prevalence of "myo-endothelial" junctions *in vivo*. These data yield further information on junctional transfer in cultured vascular endothelium and have broad implications for the functional integration of the vessel wall in the physiology and pathophysiology of the vasculature.

Key Words vascular endothelium · gap junctions · culture · dye transfer · metabolic coupling · vascular smooth muscle cells

Introduction

The distribution of intercellular junctions has been well characterized for mammalian vascular endothelium *in situ* [14, 16, 35, 36, 40, 41, 48, 49, 56]. In spite of the variability in morphology and extent of gap and tight junctions throughout the vascular tree [summarized in 50] and the potential importance of these variations in the physiology, biochemistry, and pathology of blood vessels, little work has been reported on characterization of the distribution of these structures in endothelial culture models. Endothelial cultures, derived by collagenase-dissociation of the intima of large vessels, retain many of the other characteristics of intact intimal endothelium [4, 5, 7, 11, 26, 42] and have proved to be valuable tools in modeling the vascular intima. However, we have found that the extent and complexity of gap and tight junctions are reduced in primary cultures of bovine aortic and umbilical vein endothelium [19], and others have reported apparent reductions in the frequency of gap junctions and a loss of tight junctions in serially-enzyme-passaged rabbit venous [44] and bovine arterial [38, 39] endothelial cells.

The postulated role of tight junctions in the control of trans-intimal permeability [15] and hence potentially in the pathogenesis of atherosclerosis and of gap junctions in the regulation of cell proliferation [22, 24, 46], tissue homeostasis [e.g., 23], and coordinate responsiveness to exogenous or endogenous signals [30, 31], suggests that a comparison of the physiological correlates of intercellular junctions may provide useful information in assessing data derived from experiments on cultured cells and in extrapolating back to the vessel wall.

We have previously reported the exchange of small molecules in primary cultures of bovine aortic and umbilical vein endothelial cells [19] and have provided a quantitative assessment of electrical coupling and passive membrane characteristics in these cells [18]. The present study is a more detailed, quantitative comparison of the ability of these cultures to transfer small molecules from cell to cell and a comparison of transfer in culture and in freshly isolated sheets of cells. In addition, we document and quantitate heterocellular transfer between endothelial and smooth muscle cells; a phe-

*Present address: Cardiovascular Pathology, Mallory Institute of Pathology, Boston University School of Medicine, 784 Massachusetts Avenue, Boston, MA 02118.

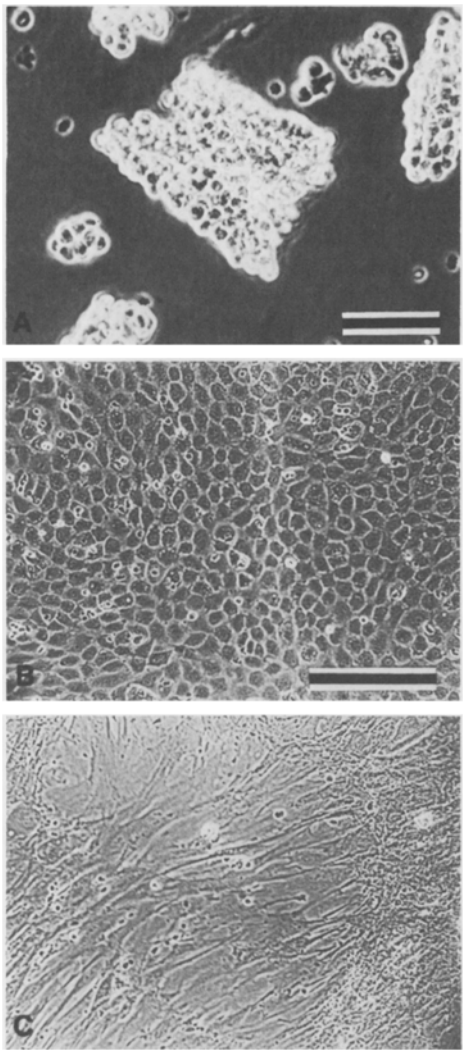

Fig. 1. Phase micrographs of vascular endothelial and smooth muscle cells *in vitro*. (*A*): Freshly isolated sheets of bovine aortic endothelial cells (BAEC). (*B*): Confluent primary culture of BAEC. (*C*): Calf umbilical vein smooth muscle cells. (Bars: (*A*) = 50 μm; (*B*) and (*C*) = 200 μm)

nomenon which may be important in the normal physiology of the vessel wall [33, 34, 47].

Materials and Methods

Cultured Cells

Calf thoracic aortae and fetal calf umbilical veins were processed for release of intimal endothelial cells by luminal collagenase treatment as previously described [18, 19]. Endothelial cells to be cultured were plated at a density of 5–7 $\times$ 10^5 cells per 60-mm plastic culture dish in Medium 199 with 30% heat-inactivated calf serum, L-glutamine, and antibiotics (all GIBCO Labs.). Cultures were maintained at 37°C in a humidified atmosphere of 95% air/5% CO_2, and the culture medium was changed every 48 hr.

Bovine aortic (BAEC) and umbilical vein (BVEC) endothelial cells, isolated by the above procedure, were released from the vessels in sheets of up to several hundred cells (Fig. 1*A*). Under culture conditions, these sheets attached to the plastic substrate and the cells flattened, migrated, and replicated. Confluent cultures were usually achieved by 3–5 days (Fig. 1*B*).

Calf umbilical vein vascular smooth muscle cells (VSMC) were isolated by modifications of the explant outgrowth technique of Ross [37] as previously described [19]. VSMC culture conditions and medium were the same as for the endothelial cells with the substitution of 10% heat-inactivated fetal calf serum (GIBCO) for the calf serum. VSMC grew to the typical post-confluent "hill and valley" pattern reported for other VSMC cultures [*see* 12; Fig. 1*C*].

The mouse L929 (subline A9) fibroblast cell line [20] was used for controls in nucleotide transfer experiments. These cells were grown in DMEM with 10% heat-inactivated fetal calf serum (GIBCO).

Endothelial cells were not routinely passaged, and all experiments were carried out using freshly isolated cells or confluent primary cultures. VSMC were subcultured when the cells became confluent. L929 cells were routinely subcultured at 2–4 day intervals. In each case, dispersal of the cells was based on minimal treatment with trypsin-EDTA followed by tituration. Cell counts were made by hemacytometer.

Dye Transfer

Freshly isolated sheets and 3–5 day confluent primary cultures of BAEC and BVEC were tested by standard methods [2, 19, 45] for the ability to transfer the fluorescent dye Lucifer Yellow CH (mol wt 457.3; supplied by W. Stewart; [52]) from cell to cell. Dye-injecting electrodes were glass micropipettes (Omega Dot, F. Haer) filled from tip to shoulder with Lucifer Yellow CH (4% in distilled water) and in the barrel with 1 M LiCl by the fiber-fill method [53]. The saline-filled micropipettes were connected to the amplifier/stimulator circuits by Ag/AgCl wires. All experiments were performed with cells at room temperature and atmosphere in phosphate-buffered saline [PBS (in mM) 137, NaCl; 2.7, KCl; 0.7, $CaCl_2$; 0.5, $MgCl_2$; 1.5, KH_2PO_4; 7.9, Na_2HPO_4, pH 7.4).

Freshly isolated cell sheets were washed once by centrifugation, resuspended in PBS, and plated out into 60-mm culture dishes. Large sheets (>200 cells) were selected under white light, dark-field illumination (Leitz Labolux II). The dye-filled electrode was then positioned over a cell in the center of the sheet. Iontophoretic ejection of dye (hyperpolarizing current pulses of 5 $\times$ 10^{-9} A, 200 msec, 1/sec) and penetration of a cell commenced under ultraviolet illumination (200 W mercury lamp; BG-12 and K-510 filters). Injection was continued for 60 sec at which time the electrode was removed from the cell.

Confluent primary cultures in 60-mm dishes were rinsed twice with PBS to reduce background fluorescence due to the culture medium. Homogeneous areas of cultures were selected for injection in order to reduce the possibility of inclusion of contaminating nonendothelial cells and to simplify interpretation of transfer. The injection protocol was as described above.

Thirty seconds after cessation of injection, a dark-field fluorescence micrograph was taken of each penetration (Tri-X, 135, Kodak; 10 sec exposure). The films were processed in Acufine (Acufine, Inc.) for an effective ASA of 1200. The resultant photo-

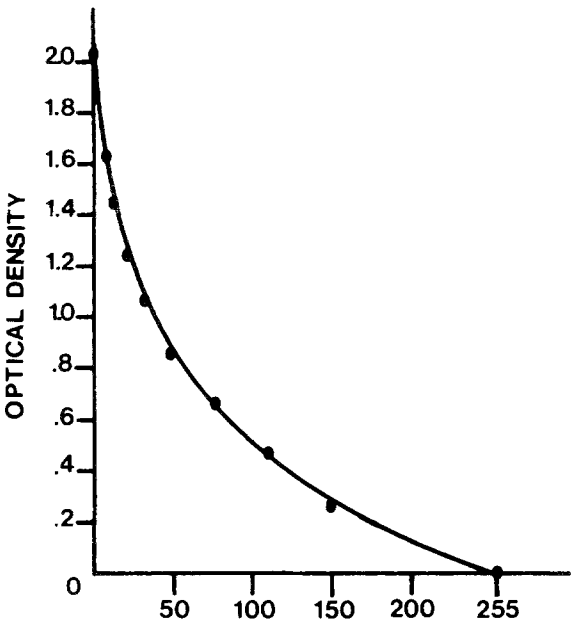

Fig. 2. Calibration curve for converting intensity (Z) values into optical densities (O.D.) for dye transfer experiments (*see* text). The experimentally determined points are fit by the equation: O.D. = $-0.0101613 - 1.31171 \log[(Z + 7)/262]$

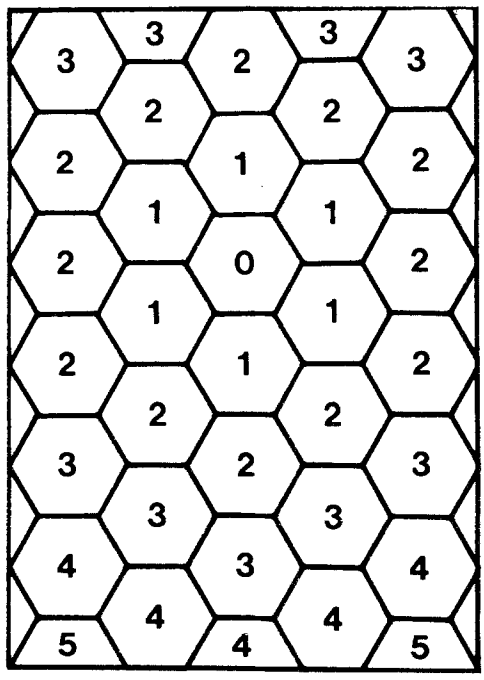

Fig. 3. Hexagonal endothelial cell packing model for dye and nucleotide transfer experiments (*see* text). Numerals are cell ranks with the injected or donor cells having rank = 0. The use of a hexagonal cell model was justified by determining the number of adjacent cells in freshly isolated sheets and in confluent primary cultures (in each case, approximately 90% of the cells counted had six adjacent neighbors; ref. 18)

graphic negatives were back-lit and imaged by a vidicon television camera (Eye Com Scanner; Spatial Data Systems) at a standard magnification and lens aperture. The video signal was digitized and stored by a Spatial Data Systems 108PTS in conjunction with a Digital Equipment PDP-11 minicomputer.

The total intensity range of the video signal was digitized in 256 equal steps (logarithmic ratio intervals). In order to provide a constant reference and to standardize the negatives, upper and lower intensity limits were set and a calibration curve was constructed. The camera was focused on an unexposed segment of developed film (background) and this intensity was set at 255. The zero intensity level was set with the number 10 step (O.D. = 2.03) of a density step wedge (Macbeth TD404A, PN29002670) over the film. The minimum intensity (greatest density) from any negative was always greater than this zero value. The intensity levels corresponding to the other steps on the density wedge were determined and a plot of optical density (O.D.) on intensity (Z) was constructed (Fig. 2). The points on this plot were fit by regression to an equation of the form: O.D. = $a + b \log x$, where $a = -0.0101613$, $b = -1.31171$, and $x = (Z + 7)/262$ ($r^2 = 0.99854$). This calibration curve is shown in Fig. 2.

The photometric accuracy (manufacturer's specifications) was ±0.02 O.D. units over the field of view and useful range of the camera (2.3 O.D.). Distance resolution was 1 pixel or approximately 1 μm (in the culture dish).

Seventy-eight negatives were imaged and digitized. The center cell (into which dye had been injected) was given a zero distance value. An intensity measurement was made at the center of the nucleus of each resolvable cell image on the negative. Each intensity measurement corresponded to a one pixel square. The intensity values were translated into relative optical densities by substitution into the above calibration equation. The distance from the center cell for each analyzed point was calculated in micrometers. In addition, the cell rank of each analyzed cell was determined. This value was the number of cells, in the most direct path, from the injected cell (based on a hexagonal packing model, reference 18; *see* Fig. 3 and legend). The combined data of optical density, distance, and cell rank were used to describe dye transfer in these cells.

Nucleotide Transfer

Cultured endothelial cells were also tested for the ability to transfer radio-labeled molecules derived from exogenously applied tritiated uridine [19]. Uridine-nucleotide transfer experiments were conducted by using the general techniques of Pitts and Simms [32] with modifications similar to those of Pederson, et al. [29] and Lo and Gilula [21].

"Donor" VSMC were labeled for 4 hr with 10–15 μCi/ml of ^{3}H-5-Uridine (New England Nuclear) in VSMC medium. These cells were then thoroughly washed with PBS to remove extracellular label and dissociated by minimal treatment with trypsin-EDTA. The cells were washed by centrifugation to remove trypsin, suspended in endothelial medium, and plated onto confluent monolayers of endothelial cells ("recipients," in 35-mm tissue culture dishes) at a ratio of 1 : 1000 (donors/recipients). This low ratio was employed to provide wide separation of donor cells, which allowed spread of uridine-derived molecules in the monolayer without ambiguous overlap of the fields of different donors. After 4 hr of incubation (37°C), the co-cultures

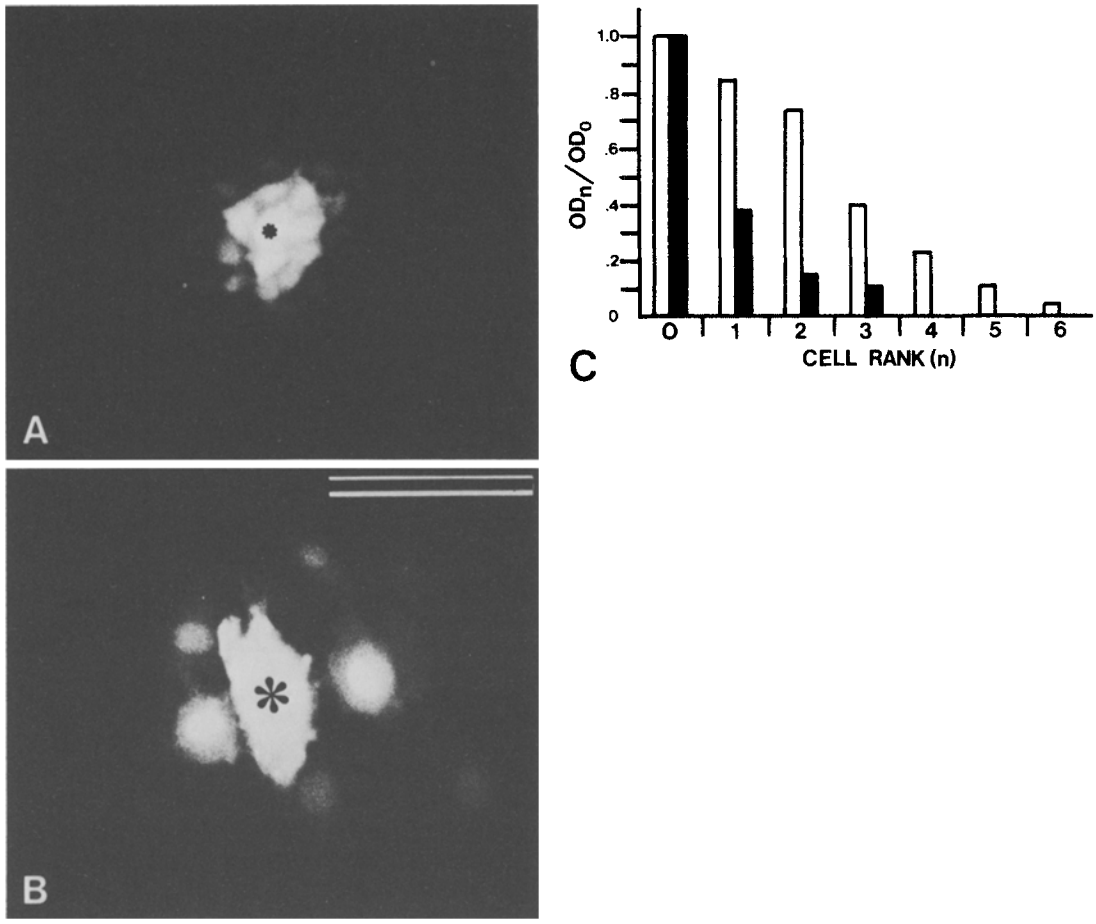

Fig. 4. Dye transfer between aortic endothelial cells. (*A*): Freshly isolated sheet of cells. (*B*): Confluent primary culture. (Asterisks = cells into which dye was injected (rank = 0, *see* text); Bar = 50 μm.) (*C*): Example of a plot of mean relative optical density ($O.D._n/O.D._0$) versus cell rank (*n*). Open bars in *C* denote a freshly isolated sheet of cells (as in *A*); solid bars denote confluent primary culture (as in *B*)

were washed thoroughly with PBS and fixed with cold 5% trichloroacetic acid. This treatment fixed the RNA in the cells and therefore allowed detection of labeled nucleotides incorporated into macromolecules. Since the uridine was tritiated in the 5 position, radiolabeled breakdown products were not retained during fixation. The fixed, co-cultured cells were processed for autoradiography using NTB-2 liquid nuclear track emulsion (Kodak) and exposed at 4°C. Autoradiograms were developed using D-19 developer (Kodak). These dishes were coverslipped with glycerin jelly and examined under phase and bright-field illumination. Grain counting was carried out according to the protocols of Pederson et al. [29] under bright-field illumination at a 100× objective magnification (oil-immersion). Grains over individual cells were counted and compared with the number of grains over cells not in contact (direct or indirect) with potential donors, cells near L929 "donors" (*see* below), and over comparable areas without cells (in subconfluent cultures). The cut-off for considering labeling to be background was the 95th percentile of the background grain distribution.

In these parallel controls, the mouse fibroblast cell line L929 (20; subline A9) was used as "recipients" or "donors." These cells have been used as a standard control for nonjunctional transfer artifacts [30] since they do not normally form gap junctions [10]. However, it has been recently shown [1] that another L929 subline (Cl-1D) is capable of forming gap junctions and engaging in electrical coupling and dye transfer under conditions known to raise intracellular cyclic AMP.

Results

Dye Transfer

Homogenous monolayers (3 to 5 days in culture) and freshly isolated sheets of endothelial cells were used to demonstrate the transfer of the fluorophore Lucifer Yellow CH. The initiation of injection of this dye into a cell was usually rapidly followed by detection of dye in adjacent cell. However, in approximately 20% of the injections attempted in cultured cells and approximately 10% for the sheets,

no transfer was seen. This failure to detect dye movement into adjacent cells probably reflected damage to the injected cells since, in most cases, the fluorescent intensity in these cells rapidly diminished upon cessation of injection (indicating leakage through disrupted plasma membranes).

At least 15 photographic negatives of successful dye transfer experiments for each of the four categories of cells (BAEC and BVEC, freshly isolated sheets and cultured cells) were analyzed as described above. In each of the cases, transfer of Lucifer Yellow into adjacent cells was detected. Figure 4 contains examples of fluorescence micrographs of dye transfer in sheet (*A*) and cultured (*B*) cells derived from bovine aortae (the asterisk denotes the cell into which dye was injected).

It is clear, from examination of the micrographs in Fig. 4, that the passive diffusion of Lucifer Yellow in the monolayers and sheets was discontinuous. One of the major discontinuities was an apparent concentration of fluorescence in the cell nuclei. The increased thickness of these cells in the perinuclear region [18, 19] was not sufficient to explain this observation. One possible explanation of this phenomenon is that the nucleoplasm has a higher water content than the general cytoplasm and therefore the dye is more soluble (higher volume concentration) in the nucleus. Alternatively, the dye molecules may have noncovalently associated with nuclear constituents. This potential association was certainly readily reversible since, in disrupted cells, all detectable dye was rapidly lost from both nucleoplasm and cytoplasm. The concentration of dye in the nucleus coupled with its central placement in these cells provided a convenient reference point for measurement.

Another major discontinuity was observed to exist at the interface between cells. Since the nonjunctional cell membrane is relatively impermeable to Lucifer Yellow CH [52] due to the charge density of the dye, the flux from cell to cell was most likely due to permeable junctions between the cells. However, diffusion within any given cell was so rapid as to be visually undetectable and so the discontinuity in fluoresent intensity at the borders between cells was also due to the junctions. Since the major barriers to radial diffusion were the interfaces between cells, the number of such barriers was clearly more critical than the distance in determining the extent of detectable transfer, at least at short times. This latter point, coupled with the demonstrable hexagonal distribution of the cells (*see* above) lead us to consideration of the monolayers and sheets as concentric ranks of cells (Fig. 3). The injected cells were given rank zero, the immediately adjacent cells rank one, etc.

Under injection and photographic conditions which were kept as constant as possible (*see* Methods), dye was photographically detected in an average of 22.8 ± 14.0 (SD) BVEC in sheets (15 negatives) per injected cell out to an average of 3.6 ± 1.1 cell ranks. For BAEC sheets (17 negatives), the corresponding means were 20.7 ± 12.6 and 3.8 ± 1.4. In the cultured cells, dye was detected in far fewer cells and fewer ranks. The averages for BVEC cultures (21 negatives) were 7.6 ± 4.4 cells and 1.8 ± 0.7 and for the BAEC cultures (25 negatives), 11.2 ± 6.4 and 2.6 ± 0.9. In addition, dye transfer to adjacent cells was always more rapidly detectable in the freshly isolated sheets than in the cultured cells (data not shown). Considering only these observations, the sheet cells would appear to have the greater transfer capabilities. However, the differences in cellular geometry between the rounded, sheet cells and the flattened, cultured cells and the potential variability in the total amount of dye injected require a more detailed analysis.

In order to control for some of this variability, the mean optical density for each cell rank ($= n$) in each negative was divided by the optical density of the $n = 0$ (injected) cell. This treatment normalized the data for cellular thickness and, hence, the major discrepancy between the geometries of the sheet and cultured cells as well as normalizing for the total amount of dye injected. When the normalized data were examined, we found that the fall-off of dye intensity with increasing cell rank from the injected cells was still greater in the cultured cells than in the sheet cells (Fig. 4*C* shows an example of this difference for the two micrographs in Fig. 4*A* and *B*). In order to put these observations on a quantitative basis, we enumerated the cell ranks at which the mean $O.D._n/O.D._0$ fell below 0.5 for each experiment. The over-all means for each data set (cultured and sheet, BAEC and BVEC) are presented in the Table.

Several control considerations must be kept in mind in interpretation of these data. First, as a check on the impermeability of plasma membranes to Lucifer Yellow, dye was iontophoretically ejected into the extracellular space, close to the cells, both above and below the endothelial monolayers and sheets. None of these tests resulted in detectable uptake of dye into cells. Second, it is important to keep in mind that the response of photographic film to light is nonlinear. This consideration was ameliorated by using strictly comparative measures of the optical density of the film. That is, comparisons were always made between frames treated as exactly equally as possible. Third, care had to be taken to ensure that saturation of the film did not cause significant loss of information at the

Table. Mean cell ranks (n) at which the normalized optical density ($O.D._n/O.D._0$) fell below 0.5000 in the dye transfer experiments

Cell type	n(mean ± SD)
Cultured cells	
BAEC	$1.20 \pm 0.41^{a,b}$
BVEC	$1.05 \pm 0.22^{c,b}$
Cell sheets	
BAEC	$1.71 \pm 0.59^{a,d}$
BVEC	$2.00 \pm 0.65^{c,d}$

[a,c] Values indicated by the same symbol are significantly different (t test: [a] $P < 0.01$; [c] $P < 0.001$).
[b,d] Values indicated by the same symbol are not significantly different.

upper end of the density range. In each of these experiments, the most dense digitized point was always less dense than fully saturated film. The final consideration is that these results are a static representation of a dynamic process (diffusion), and as such, present an arbitrary integration over a range of the time axis. Again, the use of comparative measures on equally treated material should have reduced this problem.

Nucleotide Transfer

Nucleotide transfer, as an assay for junctional transfer, is qualitatively different from the dye transfer experiments described above since the "donor" cells accumulate and phosphorylate ^{3}H-uridine naturally [13], providing a relatively impermeant (vis-à-vis nonjunctional cell membranes) nucleotide tracer. Diffusion between cells (via junctions) provides tritiated nucleotides for incorporation into acid-precipitable RNA in both the "donor" and "recipient" cells. An example of an autoradiogram resulting from such an experiment using a VSMC donor and a BVEC recipient monolayer is presented in Fig. 5. A readily discernable gradient of decreasing grain density can be seen from adjacent to more distant recipient cells. In addition, one can see the nucleolar labeling which is characteristic for uridine incorporation.

Four experiments each for aortic and umbilical vein endothelial recipient monolayers were examined. For each experiment, at least two identical dishes were used. For each cell type, 100 donor cells were randomly selected for quantitation purposes. In the autoradiograms used, grain densities of recipient cells adjacent to donors were never below 20 grains per cell (*see* below for controls) and almost invariably over 100 grains per cell.

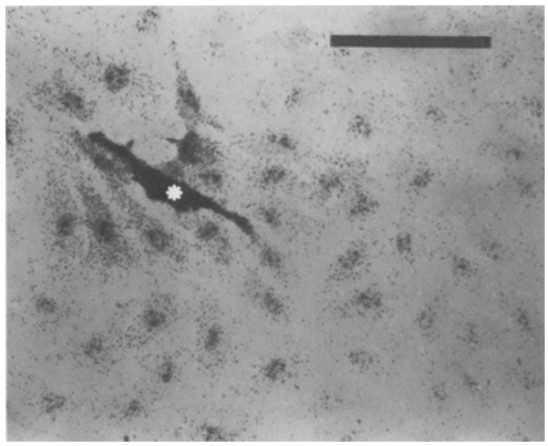

Fig. 5. Nucleotide transfer autoradiogram. Donor smooth muscle cell is denoted by asterisk. Note reduction in grain density over recipient BVEC cells with increase in cell rank. Note also nucleolar labeling characteristic of uridine labeling (Bar = 50 μm)

The extremely high grain densities of some of the recipient cells adjacent to SMC donors, coupled with the great variability of labeling in these cells under identical conditions, dictated a qualitative, comparative measure of the extent of nucleotide transfer. In analogy to the measure used in the dye transfer experiments above, the cell rank at which the grain density fell below 50% of the density of the adjacent cells (rank = 1) was enumerated. This rank number was routinely determined by estimation rather than by exact grain counting. The justifications for using an estimation procedure were that enumeration of the rank involved was only rarely ambiguous and that parallel grain counts gave the same results in 19 of 20 trials.

The mean cell rank at which this ratio (grain density_n/grain density_0) was less than 0.5 for aortic endothelial monolayers was 4.11 ± 1.03 (SD). The corresponding mean for umbilical vein endothelial monolayers was 4.05 ± 1.13. There was no significant difference between the two cell types in this parameter by t-test analysis.

For each experiment, control combinations of cells were utilized to guard against and to assess the likelihood of spurious results due to nonjunctional transfer or artifacts of the fixation or autoradiographic procedures. Figure 6 shows examples of some of the control combinations carried out in parallel for these experiments. Preloaded, trypsinized L929 cells were used as prospective donors on endothelial recipient monolayers (Fig. 6*A* and *B*). Figure 6*C* and *D* show a typical control combination of

a preloaded SMC donor on an L929 monolayer. Results of the use of L-929 "donors" and "recipients" are illustrated in Fig. 6*E* and *F*. In the controls using preloaded L929 cells on endothelial cultures, grain densities over adjacent endothelial cells rarely exceeded 20 grains per cell. A total of 100 examples of L929 "donors" was analyzed and the mean grain density over adjacent endothelial cells was 7.4 ± 3.6 (SD). When the same counts were done for 100 L929 "donors" on L929 "recipient" monolayers, the mean was 6.3 ± 4.7. This value was higher for preloaded SMC on L929 monolayers (20.6 ± 10.7). It is likely that all of these grain counts are attributable to release of small amounts of tritiated uridine (or uracil; *see* [27]) into the medium where it could be quickly taken up and incorporated into the "recipient" cells. The higher grain densities seen in the SMC/L929 combinations may mean that the SMC were more "leaky" than the L929 cells. In very rare instances, what looked like specific labeling of L929 cells at high grain densities was seen in these controls. This phenomenon is not easily explained as L929 cells do not form gap junctions or engage in transfer under normal culture conditions [10, 30]. The detection of apparent transfer in these co-cultures may, however, be related to the metabolite transfer previously reported in these cells in long-term co-culture [6] or to the recent report [1] of junction formation and electrical coupling and dye transfer in the L929, Cl-1D line under conditions known to raise the intracellular concentration of cAMP. It is possible that we have detected a similar phenomenon and that the L929 cells are able to engage in infrequent transfer. It is also possible that occasional fusion of the SMC and L929 cells may have occurred [28]. However, this potential artifact is unlikely to have played any significant role in the co-cultures of primary endothelial and smooth muscle cells.

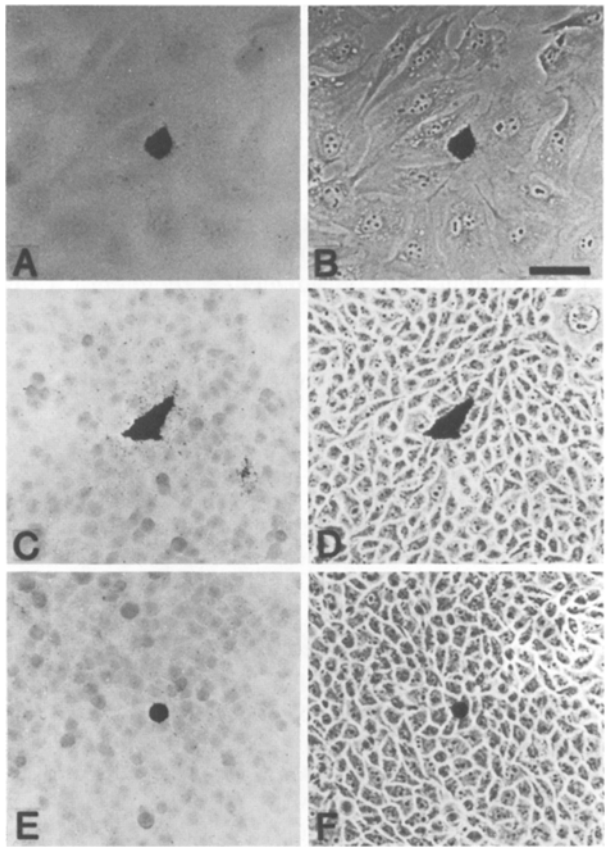

Fig. 6. Autoradiograms of control experiments for nucleotide transfer. (*A*, *C*, *E*): Bright field micrographs; (*B*, *D*, *F*): parallel phase contrast micrographs. (*A*, *B*): Labeled L929 cells as "donors" on endothelial "recipient" monolayer. (*C*, *D*): Labeled smooth muscle cell "donor" on L929 "recipients." (*E*, *F*): Labeled L929 "donor" on L929 "recipients." Parallel conditions to Fig. 5; *see* text (Bar = 50 μm)

Discussion

The purposes of this study were: (a) to determine the extent of junctional transfer of small molecular tracers in cultured vascular endothelial cells; (b) to compare the extent of such transfer in aortic versus venous cells *in vitro*; and (c) to compare the transfer characteristics of freshly isolated cells versus cells in confluent primary cultures.

Junctional Transfer in Cultured Endothelium

It is clear, from examination of fluorescence micrographs such as Fig. 4*B* and autoradiograms such as Fig. 5, that tracer molecules could be detected in adjacent ranks of cultured endothelial cells as a result of the experiments described above. The proof that these tracers pass from cell to cell via specialized membrane contacts is indirect but compelling. First, we have previously shown that gap and tight junctions exist between these cells in culture [19]. While gap junctions are thought to be the morphological counterpart of the permeable membrane channels between cells [for reviews, *see*: 17, 25], some contribution by endothelial tight junctions cannot be ruled out [47]. Second, in the case of the dye transfer studies using Lucifer Yellow CH, the charge characteristics of the tracer make it unlikely that the rapid appearance of dye in adjacent, uninjected cells could be due to leakage and reuptake [52]. Similarly, the rapid conversion of uridine into uridine phosphates in mammalian cells [13] suggests that the transferred form would be relatively (non-

junctional) membrane impermeant in these experiments as well. Third, since no significant metabolic coupling was seen in the nucleotide transfer control experiments using L929 cells as potential recipients, it is likely that specialized junctions were required. Fourth, in cases where there was release of tracer into the external environment (e.g., disruption of the membrane of the injected cell in dye transfer experiments) there was no apparent labeling of noninjected or adjacent "recipient" cells (data not shown).

Comparison of Aortic versus Venous Endothelial Cultures

Despite the differences in junctional distribution reported for arterial and venous endothelium *in situ* [e.g., 50], there appears to be little difference between the junctions of cultured aortic and umbilical vein endothelium [19] or, as we reported in a previous study [18], in electrical coupling. As we have described [19], there appears to be a normalization of the junctional extent in culture which may account for the discrepancy between cultured cells and their *in vivo* counterparts. In the initial analysis of the dye studies, we found significant differences between the aortic and venous cells both in the mean number of cells receiving detectable dye per injected cell (BAEC: 11.2 ± 6.4 vs. BVEC: 7.6 ± 4.4; $P < 0.05$) and in the mean maximum cell rank in which dye was detected (BAEC: 2.6 ± 0.9 vs. BVEC 1.8 ± 0.7; $P < 0.001$). However, these measurements of dye transfer characteristics are open to several questions due to the caveats mentioned above. When dye transfer in these cells was compared by the more rigorous normalized optical density test (cell rank (n) at which $O.D._n/O.D._0$ fell below 0.5), there was no significant difference between dye transfer in the cultured BAEC and BVEC (*see* Table). Since this latter treatment normalizes the data for variability in cellular geometry and dye injection, this test must be taken to be more indicative of the characteristics of dye transfer in these cells. Similarly, in the nucleotide transfer experiments, the rank-normalized descriptive parameter for grain density of recipient endothelial cells was not significantly different for aortic (4.11 ± 1.03) versus venous cells (4.05 ± 1.13). These experiments, together with the electrical coupling studies [18] suggest that there was no detectable difference in molecular or ionic coupling between aortic and venous endothelium in primary culture.

Comparison of Freshly Isolated versus Cultured Cells

When freshly isolated sheets of cells were tested for transfer capability using the dye injection protocols, we found that sheets from both vascular sources were clearly coupled (Fig. 4, Table). In fact, the extent of transfer in terms of numbers of cells and ranks of cells was apparently higher than in similar preparations that had been allowed to attach to the substrate and grow to confluency. However, the differences in the geometries of the sheet and cultured cells makes this comparison equivocal. When the data from the dye transfer experiments were normalized for the variability in experimental conditions (e.g., amount of dye injected) and for cell thickness (the most critical geometric factor) by the method described above, it was determined that the decrease of dye intensity with cell rank was still less in the freshly isolated sheets (significance of differences between cultured and sheet cells: BAEC, $P < 0.01$; BVEC, $P < 0.001$; *see* Table). As was the case with the cultured cells, we found no significant difference between dye transfer in BAEC and BVEC sheets using this method.

There is additional, indirect, information that bears on the difference in coupling between cultured cells and sheets. As noted above, the topology of the confluent cultured endothelium and the freshly isolated sheets is well approximated by a hexagonal array (approx. 90% of cells have six adjacent neighbors, [18]). However, in many experiments, dye transfer was detected with fewer than six rank 1 cells and the pattern of spread was often heterogenous (*see* Fig. 4*B*). In fact, the mean number of cells in rank 1 receiving detectable dye was significantly less ($P < 0.02$) in the cultures (BAEC, 4.76 ± 1.36; BVEC, 4.62 ± 1.32) than in the sheets (BAEC, 5.59 ± 0.71; BVEC, 5.53 ± 0.74). Transfer to fewer than the model six rank 1 cells implies that relatively more dye is available to those cells that are coupled. Similarly, more dye is available for transfer to cells in ranks 2, 3, etc. Since our measure of the decline of dye intensity with cell rank considered only coupled cells, we actually over-estimated dye transfer in the cultured cells in comparison to the sheet cells.

It was not technically possible to examine nucleotide transfer in freshly isolated sheets for a similar comparison with cultured cells. However, we did carry out a series of preliminary experiments using ^{3}H-uridine-prelabeled endothelial cultures (subconfluent, at one day in culture) upon which freshly isolated sheets of cells were plated. After a co-incubation period of 12–18 hr, these cultures were processed for autoradiography as above. It was clear that transfer of labeled molecules occurred essentially from prelabeled donor cells to sheets as a whole. That is, either all cells in a "recipient" sheet were labeled (with equal grain densities) or none were. Hence, the limiting factor seemed to be the establishment of competent junctions; this was followed by rapid loading of the nu-

cleotide pools of the sheet cells (data not shown; *see* [19]). Due to the extreme variability of transfer with this experimental protocol, further studies were not pursued. Clearly, however, the sheets of freshly isolated endothelial cells were well coupled.

Implications

These studies were undertaken to complement a parallel series of experiments on the characteristics of electrical coupling in vascular endothelial cultures [18] in which we investigated the cell-to-cell transfer of induced membrane potential changes in confluent monolayers of bovine aortic and umbilical vein endothelial cells. In the present study, we have clearly shown that these cells are also capable of transferring iontophoretically-injected fluorescent dye molecules and metabolically-processing, transferring, and utilizing radio-labeled metabolites derived from exogenously-applied tritiated uridine. Since each of these types of assays has its own quite different potential artifacts, and necessary controls, the use of both invasive (electrical and dye transfer) and non-invasive (nucleotide transfer) protocols, together with the ultrastructural studies [19], provides a more coherent picture of junctional transfer capability in this cell type than is possible with a single approach.

The implications for the presence of patent intercellular connections in the physiology and pathology of vascular endothelium are manifold [47]. Of the major functional roles that endothelium plays in the vessel wall, one of the most important is the maintenance of a nonthrombogenic, blood compatable surface [11]. Clearly, the postulated involvement of gap junctional communication in growth control [22, 24, 46] and, hence, the preservation of the normal monolayer topology are relevant to this function. The rapid disappearance of endothelial gap junctions in the general region of a denuding injury [43], and not just in immediately adjacent cells, might be important in releasing these cells from both contact inhibition and G1 arrest [23, 24] and allowing migration and replication for regeneration of the monolayer. Completed regeneration of the endothelium in *in vivo* injury models correlates well with the reappearance of gap junctions [43, 51].

Another postulated role of gap junctions involves tissue homeostasis and the coordinate responsiveness of coupled cells to exogenous or endogenous signals [e.g., 31]. Of interest in this regard is the reported hyperpolarization of cultured endothelial cells by acetylcholine [55]. Electrical coupling of these cells [18] could act to distribute such membrane potential deflections to neighboring cells. Similarly, alterations in the concentration of ions and small molecules would be distributed throughout the population.

Recently much attention has been paid in the literature to the phenomenon of endothelium-dependent vasorelaxation as initially reported by Furchgott and Zawadzki [9]. This response, measured primarily in arterial ring or strip preparations, has been demonstrated for ACh and a variety of other vasodilators [for reviews, *see* 8, 54] and has been postulated to be due to release of arachidonic acid metabolites by endothelial cells and activation of guanylate cyclase in smooth muscle cells (to present one scenario). However, an alternative explanation may involve the presence of endothelial-smooth muscle junctions. Perusal of the electron microscopic literature on the vessel wall shows that close appositions of endothelial and smooth muscle cells are common even in the larger, elastic arteries (where cell processes extend through fenestrations in the basal lamina and internal elastic lamina) but are especially frequent in smaller arteries, arterioles and precapillary sphincters [33, 34]. At present, the detailed ultrastructure of these appositions is unknown but, since we know that endothelial-smooth muscle junctions, at least in culture (this paper), are permeable to small molecular tracers (nucleotides) and hence, presumably to the full range of ions and small molecules below approximately 1000 daltons [25], it seems quite possible that signals generated by endothelial cells, in response to various stimuli, might be transmitted to medial smooth muscle cells via such a protected, specific pathway (as previously suggested by Rhodin [33, 34] and others [3, 18, 47]).

The authors are grateful to Patricia Anaya for her excellent technical assistance on this project, to Ephraim Y. Kam and Albert C. Wallstrom for their aid in computer programming, and to Douglas Meisner and William Johnson for providing access to the densitometry equipment. This work was supported by N.I.H. grants HL06314 and HL21166.

References

1. Azarnia, R., Dahl, G., Loewenstein, W.R. 1981. Cell junction and cyclic AMP: III. Promotion of junctional membrane permeability and junctional membrane particles in a junction-deficient cell type. *J. Membrane Biol.* **63**:133–146
2. Bennett, M. V. L. 1973. Permeability and structure of electrotonic junctions and intercellular movement of tracers. *In:* Intracellular Staining in Neurobiology. S.B. Kater and C. Nicholson, editors. pp. 115–134. Springer Verlag, New York
3. Bevan, J.A., Duckles, S.P. 1975. Evidence for alpha-adrenergic receptors on intimal endothelium. *Blood Vessels* **12**:307–310
4. Buonassisi, V., Colburn, P. 1980. Hormone and surface receptors in vascular endothelium. *Adv. Microcirc.* **9**:76–94
5. Buonassisi, V., Venter, J.C. 1976. Hormone and neurotransmitter receptors in an established vascular endothelial cell line. *Proc. Natl. Acad. Sci. USA* **73**:1612–1616

6. Cox, R.P., Krauss, M.R., Balis, M.E., Dancis, J. 1973. Metabolic cooperation in putative "non-communicating" cells. *Am. J. Human Genet.* **25**:22*A*
7. D'Amore, P., Shepro, D. 1977. Stimulation of growth and calcium influx in cultured, bovine, aortic endothelial cells by platelets and vasoactive substances. *J. Cell. Physiol.* **92**:177–183
8. Furchgott, R.F. 1983. Role of endothelium in responses of vascular smooth muscle. *Cir. Res.* **53**:557–573
9. Furchgott, R.F., Zawadzki, J.V. 1980. The obligatory role of endothelial cells in the relaxation of arterial smooth muscle by acetylcholine. *Nature (London)* **288**:373–376
10. Gilula, N.B., Reeves, O.R., Steinbach, A. 1972. Metabolic coupling, ionic coupling, and cell contacts. *Nature (London)* **235**:262–265
11. Gimbrone, M.A., Jr. 1976. Culture of vascular endothelium. *Prog. Hemostas. Thromb.* **3**:1–28
12. Gimbrone, M.A., Jr., Cotran, R.S. 1975. Human vascular smooth muscle in culture: Growth and ultrastructure. *Lab. Invest.* **33**:16–27
13. Hauschka, P.V. 1973. Analysis of nucleotide pools in animal cells. *Meth. Cell Biol.* **7**:361–462
14. Hüttner, I., Boutet, M., More, R.H. 1973. Gap junctions in arterial endothelium. *J. Cell Biol.* **57**:247–252
15. Hüttner, I., Boutet, M., More, R.H. 1973. Studies on protein passage through arterial endothelium: I. Structural correlates of permeability in rat arterial endothelium. *Lab. Invest.* **28**:672–687
16. Hüttner, I., Peters, H. 1978. Heterogeneity of cell junctions in rat aortic endothelium: A freeze-fracture study. *J. Ultrastruct. Res.* **64**:303–308
17. Larsen, W.J. 1983. Biological implications of gap junction structure, distribution and composition: A review. *Tissue Cell* **15**:645–671
18. Larson, D.M., Kam, E.Y., Sheridan, J.D. 1983. Junctional transfer in cultured vascular endothelium: I. Electrical coupling. *J. Membrane Biol.* **74**:103–113
19. Larson, D.M., Sheridan, J.D. 1982. Intercellular junctions and transfer of small molecules in primary vascular endothelial cultures. *J. Cell Biol.* **92**:183–191
20. Littlefield, J.W. 1966. The use of drug-resistant markers to study the hybridization of mouse fibroblasts. *Exptl. Cell Res.* **41**:190–196
21. Lo, C.W., Gilula, N.B. 1980. PCC4azal teratocarcinoma stem cell differentiation in culture. III. Cell-to-cell communication properties. *Dev. Biol.* **75**:112–120
22. Loewenstein, W.R. 1968. Communication through cell junctions: Implications in growth control and differentiation. *Dev. Biol.* **Suppl. 2**:151–183
23. Loewenstein, W.R. 1976. Permeable junctions. *Cold Spring Harbor Symp. Quant. Biol.* **40**:49–63
24. Loewenstein, W.R. 1979. Junctional intercellular communication and the control of growth. *Biochim. Biophys. Acta* **560**:1–65
25. Loewenstein, W.R. 1981. Junctional intercellular communication: The cell-to-cell membrane channel. *Physiol. Rev.* **61**:829–913
26. Mason, R.G., Mohammad, S.F., Saba, H.I., Chuang, H.Y.K., Lee, E.L., Balis, J.U. 1979. Functions of endothelium. *In:* Pathobiology Annual 1979, Vol. 9. H.L. Ioachim, editor. pp. 1–48. Raven Press, New York
27. McGarrity, G.J., Vanaman, V., Sarama, J. 1979. Comparative studies between microbiological culture and uptake of uridine/uracil to detect mycoplasmal infection of a cell cultures. *Exp. Cell Res.* **121**:159–165
28. Nichols, D.H., Sheridan, J.D., Sheppard, J.R. 1979. Inconspicuous murine leukemia virus induced heterologous cell fusion in the interpretation of cellular and molecular interactions. *Anat. Rec.* **193**:637(*abstr.*)
29. Pederson, D.C., Sheridan, J.D., Johnson, R.G. 1980. The development of metabolite transfer between reaggregating Novikoff hepatoma cells. *Exp. Cell Res.* **127**:159–177
30. Pitts, J.D. 1972. Direct interaction between animal cells. *In:* Cell Interactions. L.G. Silvestri, editor. pp. 227–285. North Holland, Amsterdam
31. Pitts, J.D., Finbow, M.E. 1977. Junctional permeability and its consequences. *In:* Intercellular Communication. W.D. de Mello, editor. pp. 61–86. Plenum, New York
32. Pitts, J.D., Simms, J.W. 1977. Permeability of junctions between animal cells: Intercellular transfer of nucleotides but not macromolecules. *Exp. Cell Res.* **104**:153–163
33. Rhodin, J.A.G. 1967. The ultrastructure of mammalian arterioles and precapillary sphincters. *J. Ultrastruct. Res.* **18**:181–223
34. Rhodin, J.A.G. 1968. Ultrastructure of mammalian venous capillaries, venules and small collecting veins. *J. Ultrastruct. Res.* **25**:452–500
35. Roggendorf, W., Cervos-Navarro, J. 1977. Ultrastructure of arterioles in the cat brain. *Cell Tissue Res.* **178**:495–515
36. Roggendorf, W., Cervos-Navarro, J., Lazaro-Lacalle, M.D. 1978. Ultrastructure of venules in the cat brain. *Cell Tissue Res.* **192**:461–474
37. Ross, R. 1971. The smooth muscle cell: I. Growth of smooth muscle in culture and formation of elastic fibers. *J. Cell Biol.* **50**:172–186
38. Ryan, U.S., Mortara, M., Whitaker, C. 1980. Methods for microcarrier culture of bovine pulmonary artery endothelial cells avoiding the use of enzymes. *Tissue Cell* **12**:619–635
39. Ryan, U.S., Ryan, J.W. 1982. Vital and functional activities of endothelial cells. *In:* Pathobiology of the Endothelial Cell. Nossel, H.L., Vogel, H.J., editors. pp. 455–469. Academic Press, New York.
40. Schneeberger, E. E. 1981. Segmental differentiation of endothelial intercellular junctions in intra-acinar arteries and veins of the rat lung. *Circ. Res.* **49**:1102–1111
41. Schneeberger, E.E., Karnovsky, M.J. 1976. Substructure of intercellular junctions in freeze-fractured alveolarcapillary membranes of mouse lung. *Circ. Res.* **38**:404–411
42. Schwartz, S.M. 1978. Selection and characterization of bovine aortic endothelial cells. *In Vitro* **14**:966–980
43. Schwartz, S.M., Stemerman, M.B., Benditt, E.P. 1975. The aortic intima. II. Repair of the aortic lining after mechanical denudation. *Am. J. Pathol.* **81**:15–42
44. Shaklai, M., Loskutoff, D., Tavassoli, M. 1978. Membrane characteristics of cultured endothelial cells: Identification of gap junction. *Israel J. Med. Sci.* **14**:306–313
45. Sheridan, J.D. 1971. Dye movement and low-resistance junctions between reaggregated embryonic cells. *Dev. Biol.* **26**:627–636
46. Sheridan, J.D. 1976. Cell coupling and cell communication during embryogenesis. *In:* Cell Surface in Animal Embryogenesis and Development. G. Poste, and G.L. Nicholson, editors. pp. 409–447. North-Holland, Amsterdam
47. Sheridan, J.D., Larson, D.M. 1982. Junctional communication in the peripheral vasculature. *In:* The Functional Integration of Cells in Animal Tissues. J.D. Pitts and M.E. Finbow, editors. pp. 263–283. Cambridge University Press, Cambridge
48. Simionescu, M., Simionescu, N., Palade, G.E. 1975. Seg-

mental differentiations of cell junctions in the vascular endothelium: The microvasculature. *J. Cell Biol.* **67**:863–885
49. Simionescu, M., Simionescu, N., Palade, G.E. 1976. Segmental differentiations of cell junctions in the vascular endothelium: Arteries and veins. *J. Cell Biol.* **68**:705–723
50. Simionescu, N., Simionescu, M. 1977. The cardiovascular system. *In:* Histology. (4th Ed.) L. Weiss and R.O. Greep, editors. pp. 373–431. McGraw-Hill, New York
51. Spagnoli, L.G., Pietra, G.G., Villaschi, S., Johns, L.W. 1982. Morphometric analysis of gap junctions in regenerating arterial endothelium. *Lab. Invest.* **46**:139–148
52. Stewart, W.W. 1978. Functional connections between cells as revealed by dye-coupling with a highly fluorescent naphthalimide tracer. *Cell* **14**:741–759
53. Tasaki, K., Tsukahara, Y., Ito, S., Wayner, M.J., Yu, W.Y. 1968. A simple and direct and rapid method for filling microelectrodes. *Physiol. Behav.* **3**:1009–1010
54. Vanhouette, P.M., Rimelle, T.J. 1983. Role of the endothelium in the control of vascular smooth muscle function. *J. Physiol. (Paris)* **78**:681–686
55. Venter, J.C., Buonassisi, V., Bevan, S., Heinemann, S., Bevan, J.A. 1975. Hormone and neurotransmitter receptors on the intimal endothelium. *Blood Vessels* **12**:381–382
56. Yee, A.G., Revel, J.P. 1975. Endothelial cell junctions. *J. Cell Biol.* **66**:200–204

Received 23 May 1984; revised 24 August 1984